Biosynthesis of amphotericin derivatives lacking exocyclic carboxyl groups

Maria Carmody[1], Barry Murphy[1], Barry Byrne[1], Patrick Power[1], Dilip Rai[2], Bernard Rawlings[3] and Patrick Caffrey[1].

[1]Department of Industrial Microbiology, Centre for Synthesis and Chemical Biology, Conway Institute for Biomolecular and Biomedical Research, University College Dublin, Belfield, Dublin 4, Ireland.

[2]Department of Chemistry, Centre for Synthesis and Chemical Biology, Conway Institute for Biomolecular and Biomedical Research, University College Dublin, Belfield, Dublin 4, Ireland.

[3]Department of Chemistry, University of Leicester, United Kingdom.

Address correspondence to: Patrick Caffrey, Department of Industrial Microbiology, University College Dublin, Belfield, Dublin 4, Ireland. Tel.: + + 353 1 716 1396; FAX: + + 353 1 716 1183; E-mail: Patrick.caffrey@ucd.ie.

Running title: Biosynthesis of less toxic amphotericins

Amphotericin B is a medically important antifungal antibiotic that is also active against human immunodeficiency virus, leishmania parasites and prion diseases. The therapeutic use of amphotericin B is restricted by severe side effects that can be moderated by liposomal formulation or structural alteration. Chemical modification has shown that suppression of charge on the exocyclic carboxyl group of amphotericin B substantially reduces toxicity. We report targeted deletions of the *amphN* cytochrome P450 gene from the chromosome of the amphotericin-producing bacterium, *Streptomyces nodosus*. The mutant strains produced amphotericin analogues in which methyl groups replace the exocyclic carboxyl groups. These compounds retained antifungal activity and had reduced haemolytic activity.

INTRODUCTION

There are increasingly urgent requirements for new antibiotics to treat infectious disease (1). The need is especially acute with systemic fungal infections that are increasing in incidence and are often fatal (2). Of the few antifungals available at present, the most reliable is amphotericin B [**1**] (Fig. 1), a polyene macrolide synthesised by *Streptomyces nodosus* (3). Amphotericin B disrupts ergosterol-containing fungal membranes and has a broad spectrum of activity. Whereas resistance to most non-polyene antifungals has appeared rapidly, the most prevalent fungal pathogens of humans have been slow to develop resistance to amphotericin B, even after more than three decades of clinical use (4). The advantages of amphotericin B are offset by toxicity that results from low water-solubility and interactions with cholesterol in mammalian membranes. Toxicity has also prevented full exploitation of the antiviral, antiprion and antiparasitic properties of amphotericin B (3). The adverse effects of the drug can be reduced by liposomal formulation, heat-induced superaggregation or by structural alteration (5). Chemical modification has shown that suppression of charge on the exocyclic carboxyl group reduces toxicity and improves antifungal specificity (6). Further improvements have been made by derivatisation with additional sugars (7).

Substantial reduction in amphotericin B toxicity would minimise adverse side effects on patients and also allow high-dose treatment of infections by emerging fungal pathogens that are sensitive only to high concentrations of the drug. Non-toxic amphotericin analogues and formulations may also be useful in other therapeutic areas. Polyene antibiotics delay the onset of prion diseases in animal models

(8). These effects are thought to result from interactions of polyenes with cholesterol-rich membrane microdomains that contain GPI-anchored prion proteins (3, 9). Amphotericin B formulations are gaining favour for treatment of cutaneous and visceral leishmaniasis, particularly as resistance to other anti-leishmania drugs continues to increase (10). Polyenes may also become important in treatment of viral infections. Polyenes interfere with the sterol-rich membranes of enveloped viruses such as human immunodeficiency virus (HIV) (3). Whilst non-polyene drugs constitute the highly active antiretroviral therapy that effectively eliminates free virus, reservoirs of provirus must be reactivated to allow complete clearance (11). Recently, amphotericin B has been found to reactivate latent HIV in macrophages, these polyene-stimulated cells in turn induce viral reactivation in T lymphocytes (11). Amphotericin B derivatives may form part of a strategy for eradication, rather than suppression, of the virus in AIDS patients.

Although total synthesis of amphotericin B has been achieved (12), the synthetic route towards production of improved antibiotics is not economically feasible. The starting material for lipid formulation or chemical modification is amphotericin B isolated from cultures of *S. nodosus*. Recent studies on amphotericin biosynthesis in this organism have led to the possibility of obtaining non-toxic analogues as primary fermentation products (13, 14, 15).

The carbon chain of the amphotericin B macrolactone is assembled from acetate and propionate units by a modular polyketide synthase (PKS) (13). The polyketide precursor undergoes three modifications to form the final antibiotic: oxidation of a methyl branch to a carboxyl group, glycosylation with GDP-mycosamine and hydroxylation at C-8 (13). Amphotericin A [**2**], a less active tetraene (Fig. 1), is produced as a co-metabolite. The enoyl reductase domain in module 5 of the PKS is thought to be sluggish, reducing only some of the enoyl-acyl carrier protein 5 (ACP5) oligoketide intermediates, so that amphotericin A is produced as well as amphotericin B (14). The biosynthetic gene cluster contains two cytochrome P450 genes, *amphL* and *amphN* (13). Phage KC515-mediated disruption of *amphL* led to synthesis of 8-deoxyamphotericin B (15). Disruption of *amphN* was expected to block oxidation of the C-16 methyl group in the macrolactone. Subsequent glycosylation and C-8 hydroxylation would yield 16-descarboxyl-16-methyl-amphotericin B [**3**], a compound that could rival amphotericin B methyl ester [**4**] (Fig. 1), a semi-synthetic derivative with an improved therapeutic index (3). However, since homologous recombination in *S. nodosus* is unpredictable, numerous previous attempts to disrupt *amphN* were unsuccessful. Here we report the targeted deletion of this gene.

EXPERIMENTAL PROCEDURES

Genetic procedures - *Escherichia coli* XL1-Blue was used for routine cloning. *E. coli* ET 12567 was used to obtain non-methylated DNA for digestion with *Bcl* I. *S. nodosus* ATCC14899 was used as the parent strain for gene replacements. *Streptomyces lividans* 66 (John Innes strain 1326) was used as host for construction of recombinant phages.

Construction of phages KC-*DI* and KC- *ΔNM* was carried out as described previously (16, 17). PCR was used to identify recombinant phages. Oligonucleotide primers D1F [5' AAAAGATCTTGGAGAAGGCCGTCGAGG AGATCC 3'] and D1R [5' AGGACATATGTGACTTCCTCGGTCAGTC GTTTGC 3'] were used to detect recombinant phage KC-*DI* and primers NMF [5' GCGGGGATCCGAGGGTCACCAGGACCT TTGTCTTC 3'] and NMR [5' TGACAGATCTGGACCAGGAGTTCATCA CCG 3'] were used to identify KC-Δ*NM* phages. Isolation of genomic DNA and Southern hybridisation were carried out as described (14, 15).

S. nodosus lysogens were selected with thiostrepton. To obtain revertants resulting from a second cross-over recombination event, the lysogen was cultured in the absence of thiostrepton for several generations and protoplasted. Thiostrepton-sensitive revertants were identified by toothpicking individual regenerated protoplast colonies onto tryptone soya (TS) agar and onto TS agar containing thiostrepton.

Production and analysis of polyenes - For polyene production, *S. nodosus* mutants were grown on fructose dextrin soya medium as described previously (15). Four 500ml cultures were centrifuged and the sedimented

mycelium was extracted with 400ml acetone to recover the polyenes. After concentration by evaporation, polyenes were extracted from the aqueous residue with 50ml butan-1-ol. The extract was evaporated to dryness and the polyenes were dissolved in 4ml methanol. The methanol-soluble polyene sample was applied to an Amberlite XAD16 column (2.5 x 50 cm). Polyenes were recovered after isocratic elution with methanol at a flow rate of 2ml / min. Fractions were scanned in the wavelength range 250 to 450 nm and those containing the highest concentrations of polyene were pooled and concentrated by rotary evaporation. The sample was then purified by gel filtration on lipophilic Sephadex LH20 column. Batches of 2ml containing up to 6mg total polyene (the heptaene: tetraene ratio varied between 1:3 and 10:1) were applied to a Sephadex LH20 column (50 x 2.5 cm) equilibrated with methanol and eluted at a flow rate of 1ml per min. The absorption spectrum of each fraction was measured in the wavelength range 250 to 450 nm. This revealed that gel filtration partially resolved the tetraene from the heptaene. With amphotericin-derived tetraenes, reduction of the double bond between C-28 and C-29 alters the molecular shape by making the polyene chain more flexible. This could assist resolution of tetraenes and heptaenes The usefulness of Sephadex LH20 gel permeation for separating hydroxy lipids has been reported (18).

The concentrations of heptaene and tetraene solutions were determined by measuring absorbance values at 405nm and 305nm respectively. An extinction co-efficient of 161000 litres mol^{-1} cm^{-1} was used for amphotericin B and heptaene analogues. An extinction coefficient of 79400 litres mol^{-1} cm^{-1} was used for tetraene analogues of amphotericin A (13).

Electrospray mass spectrometry was performed with a Quattro Micro tandem quadrupole mass spectrometer (Waters Corporation, Micromass Ltd., Manchester UK) in positive and negative ion modes. Exact mass measurements of the analytes were determined using an online LC to a time-of-flight instrument (Waters Corporation, Micromass Ltd., Manchester UK).

N-acetylated heptaene **3** was prepared as follows. A crude polyene extract from the Δ*NM* strain containing 24 mg heptaene was dried *in vacuo*. The residue was suspended in 3 ml methanol/DMSO (2:1). Acetic anhydride (0.1ml; 1.06 mmol) was added with stirring at 0˚C for 20 minutes. The mixture was then stirred at room temperature for 1 hour. A (100 ml) volume of diethyl ether was added and the resulting polyene precipitate was sedimented by centrifugation. About 11 mg of modified heptaene was recovered. This was purified by HPLC on a Supelco silica preparative column (25 cm x 21mm, 5µm) with a gradient of 10 to 15% methanol in ethyl acetate. Approximately 5mg of *N*-acetylated heptaene **3** was obtained. This material was used for structural characterisation by NMR. Spectra were recorded on a Bruker DRX-400 instrument.

Assessment of biological activities of polyenes - Bioassays were carried out as described previously (15). *Candida albicans* was obtained from the culture collection of the Department of Industrial Microbiology, UCD. Horse erythrocytes were used to determine minimum haemolytic concentrations (MHCs). Serial two-fold dilutions were prepared from concentrated stock solutions of polyenes in methanol. A 50 µl volume of each polyene dilution was mixed with 250 µl of 2.5% (v/v) defibrinated horse blood in phosphate buffered saline. The mixtures were incubated at 37°C for 1 hour and haemolysis was assessed visually or by sedimenting unlysed erythrocytes and determining the absorbance of the supernatant fluid at 545 nm. The MHC was recorded as the lowest concentration that gave complete haemolysis.

RESULTS

Deletion of the amphDII and amphN genes - Within the amphotericin biosynthetic gene cluster, the *amphN* P450 and *amphM* ferredoxin genes are located downstream from the *amphDII* and *DI* genes that encode mycosamine synthase and mycosaminyl transferase (14). Targeted disruption of *amphN* was found to be problematic, with phage constructs failing to integrate or giving unwanted chromosomal deletions that abolished polyene production. The reasons for these failures were not understood but it was possible that the DNA sequence of the *amphN* region was only weakly recombinogenic, or that disruption of *amphN* might cause lethal accumulation of toxic polyene biosynthetic intermediates. To gain further insights, a recombinant phage was designed to integrate

into the upstream *amphDI* gene. It was anticipated that this insertion might abolish *amphN* expression through polar effects.

A 1611 bp *Bcl*I-*Pst*I fragment (nucleotides 63933 to 65544 in sequence accession AF357202) contains the 3' end of *amphDI* and the 5' end of *amphDII*. This fragment was cloned between the *Bam*HI and *Pst*I sites of the KC-UCD1 phage vector (16) to give KC-*DI* (Fig. 2A). Correct integration of this phage should leave intact copies of *amphDI* and *amphDII* in the chromosome. However, it was anticipated that the integrated prophage DNA might separate the downstream *amphDII* and *amphN* genes from their promoter which is thought to be located upstream of *amphDI* (14).

Propagation of phage KC-*DI* on *S. nodosus* yielded two thiostrepton-resistant lysogens. Genomic DNA from these strains was analysed by Southern hybridisation. The 1611 bp *Bcl*I-*Pst*I fragment is located within a 2 kb *Nco*I fragment of *S. nodosus* chromosomal DNA (nucleotides 63699 to 65712 of the amphotericin cluster). Phage integration should result in formation of new 10.6 and 3.2 kb *Nco*I fragments that contain this sequence (Fig. 2B). Southern analysis revealed that *S. nodosus DI*-1 had only the 10.6 kb band and *S. nodosus DI*-2 had only the 3.2 kb band (Fig. 2C). This indicated that deletions had occurred around the integration site in both lysogens. *S. nodosus DI*-1 produced no polyenes. Extracts from *S. nodosus DI*-2 had a UV absorption spectrum characteristic of a tetraene / heptaene mixture, with the heptaene as the major product. These extracts had antifungal activity that was approximately ten times lower than that of amphotericin B (*vide infra*).

Analysis of *S. nodosus DI*-2 genomic DNA by PCR confirmed that the *amphDII* and *amphN* genes were deleted (data shown in supplementary material, Fig. 8). The production of a heptaene by this strain suggested that the *amphK* and *amphA* polyketide synthase genes on either side of this region remained intact. The *amphL* gene is located at a distance of 3kb from *amphM* and reads in the opposite orientation. This gene was detected by PCR and was presumably still functional.

S. nodosus DI-2 lacks the *amphN* gene and was expected to be deficient in oxidation of the polyene C-16 methyl group to a carboxyl group. This strain also lacks the *amphDII* gene and should be deficient in formation of mycosamine. A heptaene-enriched fraction was partially purified by chromatography on Amberlite XAD16 and by gel filtration on lipophilic Sephadex LH20. Analysis by electrospray mass spectrometry (ESMS) revealed a compound with a mass appropriate for **5**, an amphotericin analogue with a methyl group instead of the exocyclic carboxyl, and with a neutral deoxyhexose replacing mycosamine (Fig. 3; calculated molecular mass = 894.5; observed $[M + Na]^+$ = 917.7, $[M + K]^+$ = 933.6, $[M - H]^-$ = 893.6, $[M + Cl]^-$ = 929.6). High resolution MS in negative ion mode gave 893.4943, which is consistent with the molecular formula $C_{47}H_{74}O_{16}$ (calculated exact mass = 893.4899 for $[M - H]^-$). With samples that contained tetraene, a species with a mass of 903.5 was also detected in positive ion mode and additional species with masses of 879.5 and 915.6 were detected in negative ion mode (supplementary data, Fig. 9). These masses are appropriate for **6**, the 8-deoxytetraene analogue of **5** (calculated molecular mass = 880.5; observed $[M + Na]^+$ = 903.5, $[M - H]^-$ = 879.5, $[M + Cl]^-$ = 915.6).

The production of **5** is consistent with the genotype of *S. nodosus DI*-2. Mycosamine biosynthesis is thought to involve conversion of GDP-mannose to GDP-4-keto-6-deoxymannose, a ketoisomerisation to form GDP-3-keto-6-deoxymannose and AmphDII-catalysed transamination to form GDP-mycosamine (14). The *amphDII*-deficient *S. nodosus DI*-2 is capable of synthesising either GDP-4-keto-6-deoxymannose or GDP-3-keto-6-deoxymannose. Either of these activated deoxyhexuloses could be reduced and transferred to the modified aglycone by the glycosyl transferase encoded by the intact *amphDI* gene. GDP-4-keto-6-deoxy-D-mannose reductases have been found to function in biosynthesis of GDP-D-rhamnose in other bacteria (19). It is possible that *S. nodosus* has a ketoreductase that can act on the GDP-deoxyhexulose that accumulates in the absence of AmphDII.

Previous chemical modification experiments have shown that a positive charge on the amino sugar is important for antifungal activity of amphotericin B (6). The presence of a neutral sugar is consistent with the reduced antifungal activity of the polyenes

from *S. nodosus DI*-2. These results indicated that the AmphDI glycosyl transferase shows both sugar and aglycone flexibility.

Targeted deletion of the amphN cytochrome P450 and amphM ferredoxin genes - The polyenes produced by *S. nodosus DI*-2 suggested that amphotericin analogues lacking the C-16 carboxyl groups were not toxic to the producing cell. Renewed efforts were made to achieve a targeted disruption of the *amphN* gene that would leave the glycosylation genes intact.

A 1200 base-pair *Stu* I fragment was deleted from a pUC118 plasmid clone of the 6 kb *Pst*I fragment containing the *amphN* region of the amphotericin biosynthetic gene cluster (nucleotides 58981 to 65544). This deletion removed the 3' end of the *amphN* gene, the adjacent *amphM* ferredoxin gene, and part of ORF3 which has no role in amphotericin biosynthesis (14). The ligated flanking sequences were cloned as a *Bcl*I – *Pst*I fragment into the KC-UCD1 phage vector to generate the recombinant phage KC-Δ*NM* (Fig. 4A). Propagation of this phage on *S. nodosus* yielded two thiostrepton-resistant lysogens. Analysis of genomic DNA by Southern hybridisation revealed that one of these had a correctly integrated prophage (not shown). Thiostrepton-sensitive revertants were identified by screening. Analysis of genomic DNA by PCR revealed that several had undergone gene replacement. Results from a typical deletion mutant are shown in Fig. 4B. Further analysis by Southern hybridisation revealed that the 5.3kb *Nco*I fragment containing the *amphNM* region had been replaced by a smaller 4.1 kb fragment (supplementary data, Fig. 10). The deletion mutant was designated *S. nodosus* Δ*NM*. This strain gave total polyene yields of up to 0.05g per litre in unoptimised batch cultures. Under the same growth conditions the wild type *S. nodosus* produced 1g polyene per litre. The ratio of tetraene:heptaene was variable in both strains.

Analysis of polyenes from S. nodosus Δ*NM* - Polyenes were extracted from mycelium and purified by chromatography on Amberlite XAD16 and by gel filtration on Sephadex LH20. The tetraene eluted ahead of the heptaene, so that with tetraene-rich extracts the tetraene could be separated from lower levels of heptaene. The heptaene could be purified from extracts of cultures that produced this compound exclusively. Absorption spectra of heptaene and tetraene fractions are shown in supplementary data (Fig. 11).

Analysis of the tetraene fraction by electrospray mass spectrometry revealed a major compound with a mass appropriate for **7**, 8-deoxy-16-descarboxyl-16-methyl-amphotericin A (Fig. 5; calculated molecular mass 879.5; observed $[M + H]^+$ = 880.5, $[M + Cl]^-$ = 914.6). High resolution ESMS gave the molecular formula $C_{47}H_{77}NO_{14}$ (calculated exact mass for $[M + Cl]^-$ = 914.5033, observed mass = 914.5018).

The purified heptaene fraction had a major species with a mass appropriate for **3**, 16-descarboxyl-16-methyl amphotericin B (Fig. 6; calculated molecular mass 893.5; observed $[M + H]^+$ = 894.6, $[M + Na]^+$ = 916.6; $[M- H]^-$ = 892.6, $[M + Cl]^-$ = 928.6). A dehydrated form of the heptaene was also detected ($[M + H]^+$ = 876.6), $[M - H]^-$ = 874.6). High resolution ESMS gave the molecular formula $C_{47}H_{75}NO_{15}$ (calculated exact mass for $[M – H]^-$ = 892.5058, observed = 892.5043).

It is unclear why the heptaene **3** is apparently hydroxylated at C-8 whereas the tetraene **7** is not. *S. nodosus DI*-2 also appeared to produce a heptaene **5** that is hydroxylated and a tetraene **6** that is not (*vide supra*). It is possible that the AmphM ferredoxin normally co-operates with both the AmphL and AmphN cytochrome P-450s. In the *amphNM* mutant, AmphL may recruit a different ferredoxin to form a complex that acts less efficiently on the tetraene.

Heptaene **3** was also characterised by NMR. The mycosamine amino group was acetylated to facilitate further purification. Analysis by ESMS revealed molecular ions with masses appropriate for *N*-acetylated forms of heptaene **3** ($[M + Na]^+$ = 958.5; $[M + Cl]^-$ = 970.5) (data not shown). Final purification was achieved by HPLC. Examination by proton NMR (400 MHz, d4-methanol) gave a spectrum reminiscent of that for amphotericin B with four doublets (supplementary material, figure 11). However, the integration of the upfield doublet suggested two methyl doublets. Phase sensitive proton-proton correlation spectroscopy revealed that the resonances at 1.02 were indeed two methyl doublets, correlating with 1.24 and 1.82 ppm, the latter being consistent with coupling to the C-16

proton in the expected product (Table 1; Fig. 7; supplementary material, Fig. 13). These data are consistent with the presence of a methyl group attached to C-16. The assignments are based upon the couplings observed in the COSY spectrum, and by chemical shift analogy with amphotericin B.

Biological activities of novel polyenes - Agar diffusion assays were used to test the activities of the novel polyenes against *Candida albicans*. Under the conditions used, the tetraene 8-deoxy-16-descarboxyl-16-methyl-amphotericin A [**7**] showed a minimum inhibitory concentration (MIC) of 5 µg per ml whereas amphotericin B showed an MIC of 1.25 µg per ml. The tetraene **7** was therefore four times less active than amphotericin B. However, the tetraene showed a dramatic reduction in haemolytic activity. The minimum haemolytic concentration was 166 µg per ml compared to 5 µg per ml for amphotericin B, a 33-fold reduction. The purest heptaene sample contained 16-descarboxyl-16-methyl amphotericin [**3**] and a dehydrated form of this heptaene. This mixture had an MIC of 1 µg total heptaene per ml against *C. albicans*, indicating that the antifungal activity is comparable to that of amphotericin B. The MHC was 50 µg per ml, indicating that the heptaene mixture was ten times less haemolytic than amphotericin B. Previous studies have compared the MICs and MHCs of amphotericin B, its methyl ester and various semi-synthetic derivatives (6, 20). Our results for amphotericin B fall within the range of values obtained by other groups. Slight variations in these estimates presumably result from differences in assay conditions. However, our results indicate that the new analogues **3**, **5** and **7** have antifungal activities that are comparable to that of amphotericin B whereas their haemolytic activities are lower.

DISCUSSION

The biosynthetic gene clusters for a number of polyenes have now been investigated. These include amphotericin (14), nystatin (21), candicidin/FR-008 (22, 23), pimaricin (24) and rimocidin (25). All of these clusters contain cytochrome P450 genes homologous to *amphN*. These P450s are thought to function in formation of the exocyclic carboxyl group that is characteristic of most glycosylated polyenes (26). The amphotericin, nystatin and pimaricin clusters contain additional P450 genes (*amphL*, *nysL* and *pimD*). The AmphL, NysL and PimD P450s are homologous to each other and are thought to act on the polyol chains of their respective polyene macrolactones. Inactivation of *pimD* resulted in formation of 4,5-de-epoxypimaricin (27) whereas inactivation of *amphL* resulted in formation of 8-deoxyamphotericin B (15).

Here we show that deletion of *amphN* and *amphM* results in formation of novel polyenes with masses appropriate for analogues in which the C-16 methyl group is not oxidised.

Modification of the exocyclic carboxyl group of amphotericin B is known to bring about a substantial reduction in its toxicity (6). When the polyene interacts with membrane sterols, this carboxyl group is thought to contribute to an extensive network of hydrogen bonds that involves the mycosamine amino group, a water molecule and the sterol hydroxyl group (28). This system of bonds is equally strong in polyene-cholesterol and polyene-ergosterol complexes. With amphotericin B methyl ester, this network is weakened, so that the polyene binds more selectively to ergosterol through specific hydrophobic interactions within the lipid bilayer. The amphotericin analogues **3** and **7** are expected to show similar improvements in specificity as the C-16 carboxyl groups are replaced by methyl groups. Here we show that these compounds retain good antifungal activity and have lower haemolytic activities than amphotericin B.

It is unclear why the yields of these new analogues are lower than that of amphotericin B. However, further strain improvement could lead to production of these compounds on a larger scale to provide material for further chemical modification or lipid formulation.

In addition, our results establish the role of the AmphN protein in amphotericin biosynthesis. AmphN is unusual among the cytochrome P450s that modify macrolide antibiotics in that it appears to introduce two oxygen atoms into an unactivated methyl group. Directed evolution could alter the substrate specificity of this enzyme to allow further diversification of polyketide libraries in combinatorial biosynthesis.

Acknowledgements - This work was supported by grants to P. Caffrey from the European Union (GENOVA QLRT-1999-00095) and from the Irish Higher Education Authority Programme for Research in Third Level Institutions (PRTLI cycle 3).

REFERENCES

1. Walsh, C. (2003) *Nature Reviews Microbiology* **1**, 65 – 70

2. Georgopapadakou, N. H. and Walsh, T. J. (1996) *Antimicrob. Agents. Chemother.* **40**, 279 –291

3. Hartsel, S., and Bolard, J. (1996) *Trends Pharm. Sci*. **17**, 445 – 449

4. Masia. M., and Gutierrez, F. (2002) *The Lancet infectious diseases* **2**, 550 – 563

5. Lemke, A., Kiderlen, A. F., and Kayser, O. (2005) *Appl. Microbiol. Biotechnol.* Available online DOI 10.1007/S00253-005.1955-9

6. Cheron, M., Cybulska, B., Mazerski, J., Gryzbowska, J., Czerwinski, A., and Borowski, E. (1988) *Biochem. Pharmacol*. **37**, 827 – 836

7. Szlinder-Richert, J., Mazerski, J., Cybulska, B., Grzybowska, J., Borowski, E. (2001) *Biochim. Biophys. Acta* **1528**, 15 – 24

8. Pocchiari, M., Schmittinger, S., and Masullo, C. (1987) *J. Gen. Virol.* **68**, 219 – 223

9. Mange, A., Milhavet, O., McMahon, H. E. M., Casanova, D., and Lehmann, S. (2000) *J. Neurochemistry* **74**, 754 - 762

10. Gaboriou, F., Cheron, M., Petit, C., Bolard, J., and Croft, S. L. (1999) *Antimicrob. Agents Chemother*. **43**, 390 – 392

11. Jones, J., Kosloff, B. R., Benviste, E. N., Shaw, G. M., & Kutsch, O. (2005) *Virology* **331**, 106 – 116

12. Nicolaou, K. C., Daines, R. A., Ogawa, Y., and Chakraborty, T. K. (1988) J. Am. Chem. Soc. **110**, 4696 – 4705

13. McNamara, C. M., Box, S., Crawforth, J. M., Hickman, B. S., Norwood, T. J., Rawlings, B. J. (1998) *J. Chem. Soc. Perkin* **1**, 83 – 87

14. Caffrey, P., Lynch, S. V., Flood, E., Finnan, S., and Oliynyk, M. (2001) *Chem. Biol.* **8**, 713-723

15. Byrne, B., Carmody, M., Gibson, E., Rawlings, B., and Caffrey, P. (2003) *Chem. Biol.* **10**, 1215 – 1224

16. Carmody, M., Byrne, B., Murphy, B., Lynch, S., Flood, F., Finnan, S., and Caffrey, P. (2004) *Gene* **343**, 107 – 115

17. Kieser, T., Bibb, M. J., Buttner, M. J., Chater, K. F., and Hopwood, D. A. (2000) *Practical Streptomyces Genetics*. John Innes Foundation, Norwich, United Kingdom.

18. Calderon, M., and Baumann, W. J. (1970) J. Lipid. Res. 11, 167 -169

19. Maki, M., Jarvinen, N., Rabina, J., Roos, C., Maaheimo, H., Renkonen, R. (2002) *Eur. J. Biochem.* **269**, 593 – 598

20. Taylor, A. W., Costello, B. J., Hunter. P. A., MacLachlan, W. S., and Shanks, C. T. (1993) *J. Antibotics* **46**, 486 - 493

21. Brautaset, T., Sekurova, O. N., Sletta, H., Ellingsen, T. E., Strom, A. R., Valla, S., and Zotchev, S. B. (2000) *Chem. Biol*. **7**, 395 - 403

22. Campelo, A. B, and Gil, J. A. (2002) *Microbiol*. **148**, 51 - 59

23. Chen, S., Huang, X., Zhou, X., Bai, L., He, J., Jeong, K. J., Lee, S. Y., and Deng, Z. (2003) *Chem. Biol*. **10**, 1065 – 1076

24. Aparicio, J. F., Fouces, R., Mendes, M. V., Olivera, N., and Martin, J. F. (2000) *Chem. Biol*. **7**, 895 - 905

25. Seco, E. M., Perez-Zuniga, F. J., Rolon, M. S., and Malpartida, F. (2004) *Chem. Biol*. **11**, 357 - 366

26. Omura, S, and Tanaka, H. (1986) In *Macrolide antibiotics, Chemistry, Biology and Practice*. (Omura, S., ed.) pp. 351 – 404, Academic Press, New York

27. Mendes, M. V., Recio, E., Fouces, R., Luiten, R., Martin, J. F., and Aparicio, J. F. (2001) *Chem. Biol*. **8**, 635 - 644

28. Herve, M., Debouzy, J. C., Borowski, E., Cybulska, B., and Gary-Bobo, C. M. (1989) *Biochim. Biophys. Acta* **980**, 26 – 272

FOOT NOTES

Abbreviations used are: HIV, human immunodeficiency virus; AIDS, acquired immunodeficiency syndrome; PKS polyketide synthase; ESMS, electrospray mass spectrometry; NMR, nuclear magnetic resonance; COSY, correlation spectroscopy; MIC, minimum inhibitory concentration; MHC, minimum haemolytic concentration.

The term “tetraene” is used to describe amphotericin A and derivatives in which the C-28 – C-29 double bond is reduced. Amphotericin B and derivatives with a series of seven conjugated double bonds are described as heptaenes.

Figure 1. Structures and masses of amphotericins B and A and analogues. These compounds are: **1**, amphotericin B; **2**, amphotericin A; **3**, 16-descarboxyl-16-methyl-amphotericin B; **4**, amphotericin B methyl ester; **5**, 16-descarboxyl-16-methyl-19(O)-(6-deoxyhexosyl)-19(O)-desmycosaminyl - amphotericin B; **6**, 8-deoxy-16-descarboxyl-16-methyl-19(O)-(6-deoxyhexosyl)-19(O)-desmycosaminyl- amphotericin A; **7**, 8-deoxy-16-descarboxyl-16-methyl amphotericin A. The monoisotopic masses used to calculate molecular masses were: H = 1.0078; C = 12.000; O = 15.994; N = 14.0067. All double bonds represented by X-Y are *trans*.

Figure 2. Integration of recombinant phage KC-*DI* into the *amphDI* region.
A. The insert in phage KC-DI is a 1611 bp fragment that contains the 3' end of *amphDI* and the 5' end of *amphDII*. Homologous recombination between phage and chromosomal DNA inserts a prophage between the intact *amphDI* and *amphDII* gene sequences. *S. nodosus* lysogens are obtained by selecting for a thiostrepton-resistance gene within the prophage genome.
B. Strategy for analysis of lysogens by Southern hybridisation. The *Bcl*I-*Pst*I sequence is drawn as a white rectangle. Heavy black lines represent *Nco*I fragments that incorporate this sequence. Genomic DNA from a true lysogen should yield 10.6 and 3.2 kb *Nco*I fragments that hybridise to the *Bcl*I-*Pst* I fragment probe. The positions *Nco*I sites in the phage genome were obtained from (17).
C. Analysis of *Nco* I-cut genomic DNA from lysogens by Southern hybridisation with the 1611 kb *Bcl* I-*Pst*I fragment probe. The parent *S. nodosus* strain yielded the expected 2.0 kb fragment (lane 1). Lysogen *DI*-2 had the 3.2 kb fragment but not the 10.6 kb fragment (lane 2). This indicated a deletion in *amphDII* region. Lysogen *DI*-1 had the 10.6 kb fragment but not the 3.2 kb fragment (lane 3). This indicated a deletion in the *amphDI* region.

Figure 3. Analysis of polyenes produced by *S. nodosus DI*-2 by ESMS. Spectra obtained in positive and negative ion mode are shown in panels A and B respectively. All compounds show three peaks with an M: M+1: M + 2 ratio of about 6:3:1 due to isotopic natural abundance. The major peak in panel A corresponds to the sodium adduct of **5** ($[M + Na]^+ = 917.5$). This compound was also detected in negative ion mode ($[M - H]^- = 893.5$; $[M + Cl]^- = 929.5$).

Figure 4. Deletion of the *amphN* and *amphM* genes.
A. Schematic representation of recombination events between KC-Δ*NM* and the *S. nodosus* chromosome leading to targeted deletion. The insert in phage KC-Δ*NM* is a *Bcl*I-*Pst*I fragment representing nucleotides 63938 to 58981 of the amphotericin biosynthetic gene cluster (Accession number = AF357202) from which an internal 1220 bp *Stu*I fragment (nucleotides 61436 to 62667) had been deleted. This deletion from the *amphN* region is shown as a broken line. The arrows indicate the PCR primers DNMF and DNMR used to amplify the region containing the deletion.
B. Double cross-over recombinants with the required gene replacement were identified by PCR. Primers DNMF [5' GAAAGCGGGGGAAGAAGCGTCCACCAAG 3'] and DNMR [5' ATTTAGATCTGACGAGCGGATCGACGCGTTGC 3'] yielded a PCR product band of 1750 bp from *S. nodosus* genomic DNA (lane 2) and a band of 550 bp from a typical *amphNM* deletion mutant (lane 2). Lane M contains a 1kb ladder molecular size marker.

Figure 5. Analysis of tetraene produced by *S. nodosus* Δ*NM* by ESMS. A. Analysis of the tetraene fraction in positive ion mode yielded a strong peak appropriate for **7** ($[M + H]^+ = 880.5$). B. The chloride adduct of **7** was detected when the tetraene was analysed in negative ion mode ($[M + Cl]^- = 914.6$). The intensity of the M + 2 peak at 916.6 is increased as a result of the high natural abundance of ^{37}Cl relative to ^{35}Cl.

Figure 6. Analysis of the heptaene produced by *S. nodosus* Δ*NM* by ESMS. A. Analysis in positive ion mode revealed peaks with masses appropriate for **3** ($[M + H]^+ = 894.5$; $[M + Na]^+ = 916.5$). The peak at 876.5 appears to be a dehydrated form of **3**. B. Analysis of the heptaene in negative ion mode also revealed masses appropriate for 3 ($[M - H]^- = 892.5$; ($[M + Cl]^- = 928.5$). The peak at 941.6 is thought not to result from a polyene.

Figure 7. Proposed structure of **3** with the five vicinal methyl-methine coupling correlations indicated by double-headed arrows.

Supplementary material figures

Figure 8. PCR analysis of deletion in strain *S. nodosus DI*-2. A. Recombination between phage KC-*DI* and the *S. nodosus* chromosome results in insertion of prophage DNA between the *amphDI* and *amphDII* genes. The *S. nodosus DI*-2 lysogen has a deletion of the *amphDII* region. PCR was carried out to determine whether the *amphDII*, *amphN* and *amphL* genes were present. The primers used to detect these genes are indicated by pairs of arrows. B. Agarose gel electrophoresis of PCR products amplified from genomic DNA from *S. nodosus* and *S. nodosus DI*-2. Lane M: markers, 1 kb ladder; Lanes 1 and 2, products amplified from wild type and lysogen DNA, respectively, with *amphDII* primers D2F [5' GAAGTCACATATGTCCTATACGTATCCGGTC 3'] and D2R [5' TTCCAAGCTTCATCACAGGACTCCGTAGAAGGC 3']. Lanes 3 and 4, products amplified from wild type and lysogen DNA, respectively, with *amphL* primers DM1 5' AAAAAAGCTTGATGTCCTGCTGATCGGATGTGGCT 3' and
DM2 5' TACGGAGTCCTCATATGACCGCCGAGACCGAGATGACGACCTT 3'
Lanes 5 and 6, material amplified from wild type and lysogen DNA with *amphN* primers DM3 5' AAGGAGTAGCAGTCATATGGTCAACCCGACACCGCCGCC 3' and DM4 5' AAAAAAGCTTCGGTGAGCCCTTCACACTTCATG 3'.

Figure 9. Analysis of tetraene/heptaene mixture purified from *S. nodosus DI-2* in positive ion mode (panel A) and negative ion mode (panel B). The peaks at 917.5 and 893.3 correspond to **5** ($[M + Na]^+$ = 917.5; $[M - H]^-$ = 893.5). The peak at 903.5 corresponds to the sodium adduct of **6** ($[M + Na]^+$ = 903.5). **6** was also detected in negative ion mode ($[M - H]^-$ = 879.5; $[M = Cl]^-$ = 915.6).

Figure 10. Analysis of genomic DNA from *S. nodosus* Δ*NM* by Southern hybridisation. A. Schematic diagram showing approximate positions of the *Nco*I sites in the *amphN* region in *S. nodosus* and *S. nodosus* Δ*NM*. These *Nco*I sites are located at 58374, 63699 and 65712 in the sequence of the amphotericin cluster.
B. *Nco*I digests of chromosomal DNA from wild-type *S. nodosus* (lane 2) and *S. nodosus* Δ*NM* (lane 1) analysed by Southern hybridisation with a probe for the 5' end of the *amphN* gene (a *Bcl* I – *Stu*I fragment representing nucleotides 62662 to 63938 of the amphotericin cluster). The 5.3 kb *Nco* I fragment containing the *amphN* gene in wild type is replaced by a 4.1 kb fragment in *S. nodosus* Δ*NM*. The probe overlaps the downstream 2kb *Nco*I fragment by 240 base pairs. This band is visible in lanes 1 and 2.

Figure 11. Analysis of tetraene and heptaene fractions isolated from *S. nodosus* Δ*NM* by UV spectrophotometry. A. Absorption spectrum of tetraene showing peaks at 292, 305 and 320 nm. B. UV absorption spectrum of heptaene with peaks at 363, 382 and 405 nm. The tetraene fraction contains 8% heptaene.

Figure 12. Proton NMR spectrum of *N*-acetyl heptaene **3**.

Figure 13. COSY spectrum of *N*-acetyl heptaene **3**.

Table 1. Analysis of *N*-acetylated heptaene **3** by NMR. Proton chemical shifts, assignments and correlations observed by proton NMR and 2D correlation NMR spectroscopy.

Assignment	ppm	Correlations Strong/weak
39	1.02 (3H, d)	1.82
41	1.02 (3H, d)	1.24
40	1.12 (3H, d)	2.39
38	1.20 (3H, d)	5.38
16	1.24 (1H)	3.96
6’	1.26 (3H, d)	3.28
	1.30	1.97
	1.35	1.82
	1.45	4.20
	1.49	3.72
18a	1.72	4.33/3.96(3.65/3.22/2.22/1.45w)
36	1.82	1.02
	1.97 (1H)	1.30
N-Acetyl	2.02 (3H, s)	None
18b	2.22 (1H)	1.72/4.42w
	2.25 (1H)	4.20
36	2.38	3.24/5.38w
34	2.39 (1H)	1.12
	3.22 (2H)	1.72
35	3.24 (1H)	2.38
5’	3.28 (1H)	1.26/3.83
	3.61 (2H)	1.26w
	3.62 (2H)	1.72s
	3.72 (2H, ca t)	1.49
	3.78 (2H)	none
4’	3.83 (3H)	3.28
17	3.96 (2H, ca t)	1.24/1.72w
	4.20 (2H)	1.45m/2.25m
	4.33 (2H, ca t)	1.72
19	4.42 (2H, ca t)	6.03/2.22w
1’	4.61 (1H, br s)	none
33	5.38 (1H)	6.18 (H-32)
37	5.38 (1H)	1.20/2.38
31	6.01 (ca dd)	6.18 (H-32)
20	6.03 (ca dd)	4.42
21-32	6.15-6.55 (12H)	6.01/5.38

Figure 1

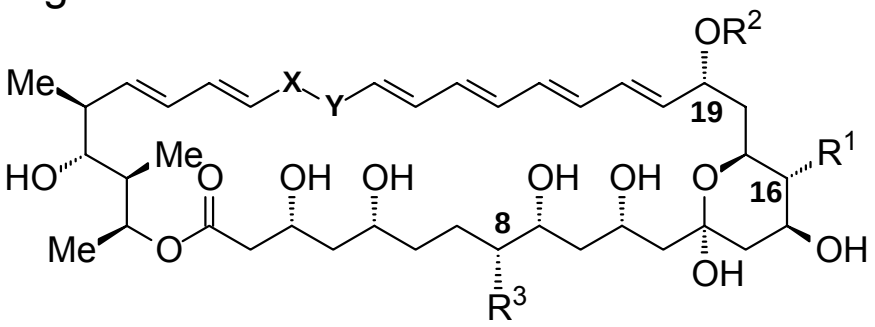

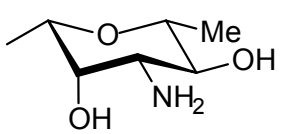

Mycosaminyl

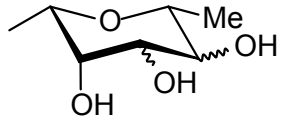

Deoxyhexosyl

	R^1	R^2	R^3	X-Y	RMM
1	-COOH	Mycosaminyl	–OH	-HC=CH-	923.5
2	-COOH	Mycosaminyl	–OH	$-H_2C-CH_2-$	925.5
3	$-CH_3$	Mycosaminyl	–OH	-HC=CH-	893.5
4	-COOMe	Mycosaminyl	–OH	-HC=CH-	937.5
5	$-CH_3$	Deoxyhexosyl	–OH	-HC=CH-	894.5
6	$-CH_3$	Deoxyhexosyl	–H	$-H_2C-CH_2-$	880.5
7	$-CH_3$	Mycosaminyl	–H	$-H_2C-CH_2-$	879.5

Figure 2

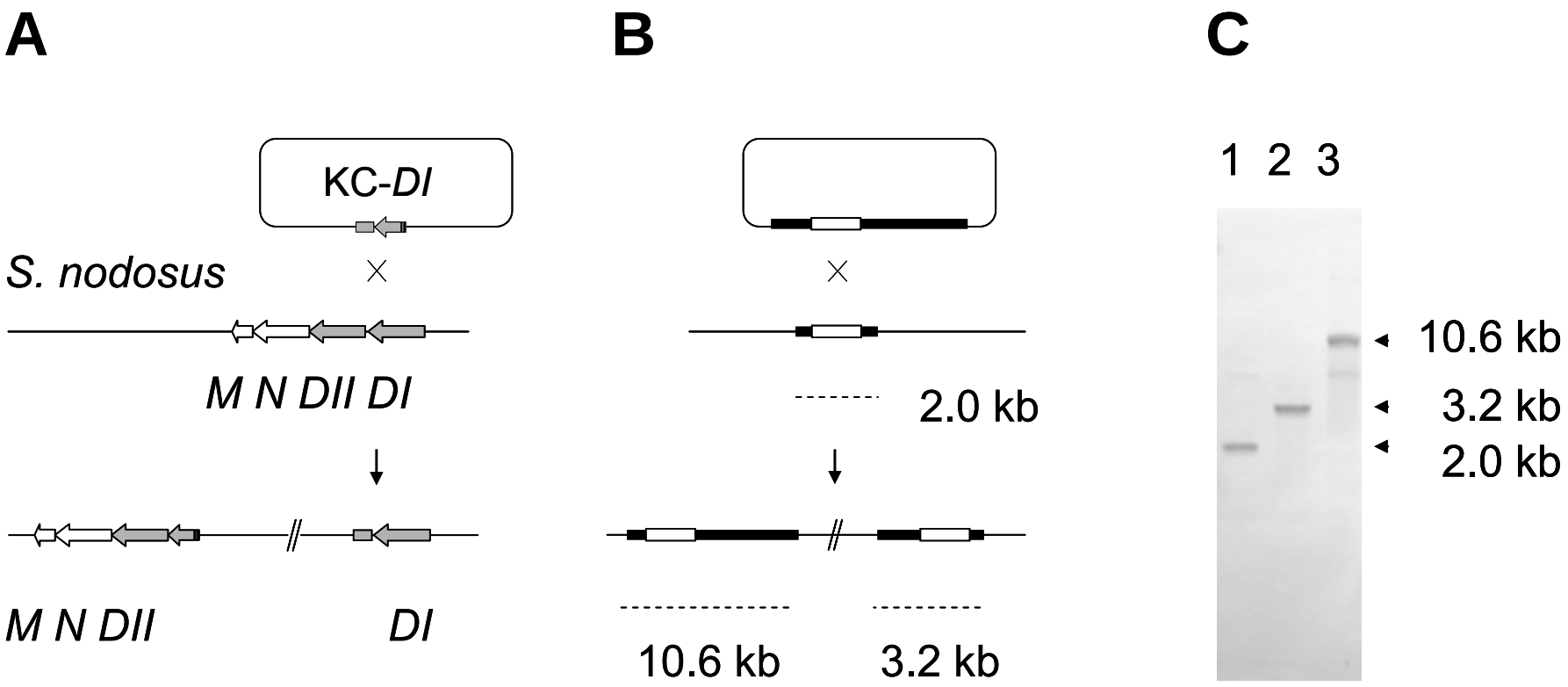
A
KC-DI
S. nodosus
M N DII DI
M N DII
DI
B
2.0 kb
10.6 kb
3.2 kb
C
1 2 3
10.6 kb
3.2 kb
2.0 kb

Figure 3

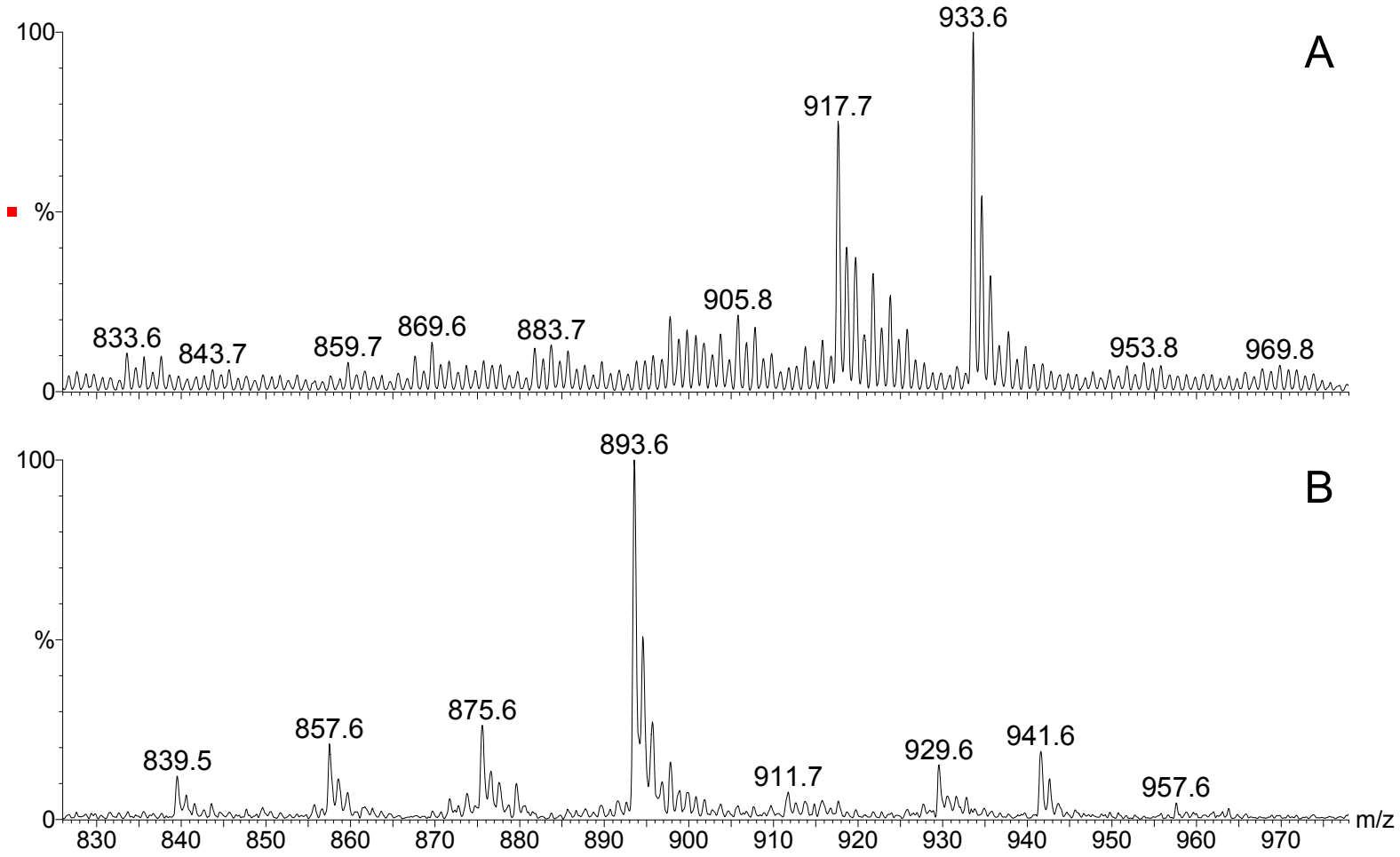
A
100
%
0
933.6
917.7
905.8
833.6
843.7
859.7
869.6
883.7
953.8
969.8
B
100
%
0
893.6
839.5
857.6
875.6
911.7
929.6
941.6
957.6
830
840
850
860
870
880
890
900
910
920
930
940
950
960
970
m/z

Figure 4

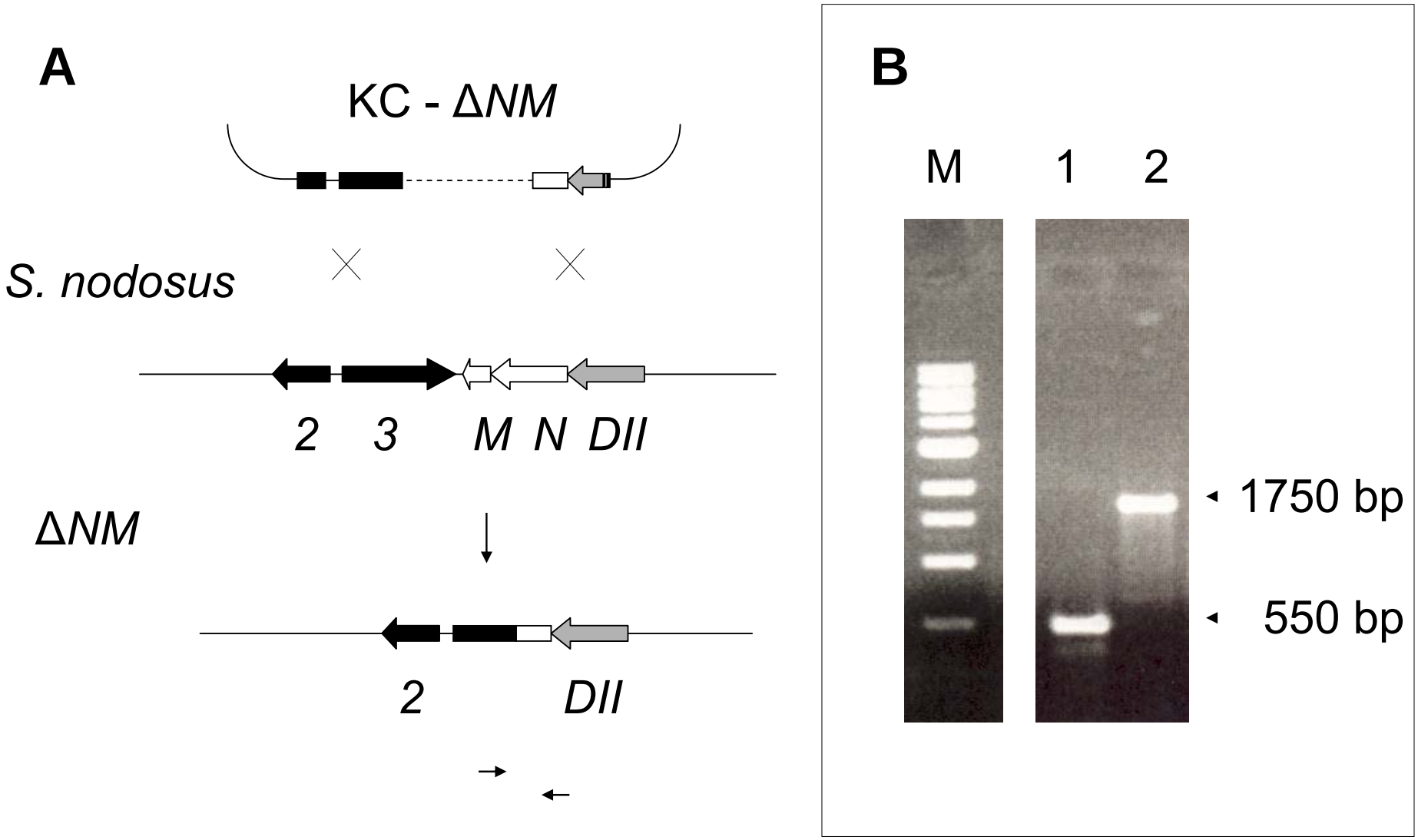

Figure 5

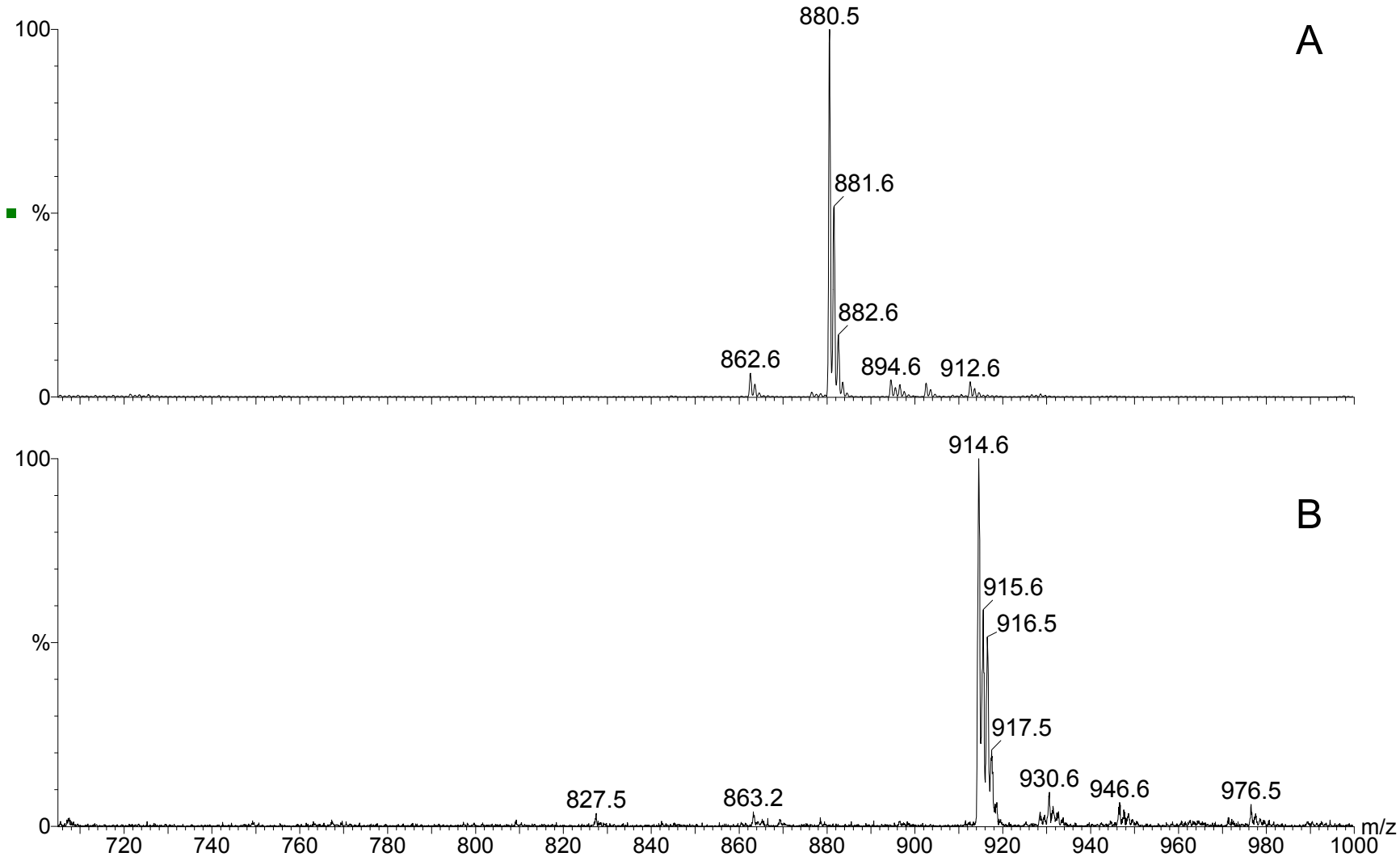
A
100
%
0
880.5
881.6
882.6
862.6
894.6
912.6
B
100
%
0
914.6
915.6
916.5
917.5
930.6
946.6
976.5
827.5
863.2
720
740
760
780
800
820
840
860
880
900
920
940
960
980
1000
m/z

Figure 6

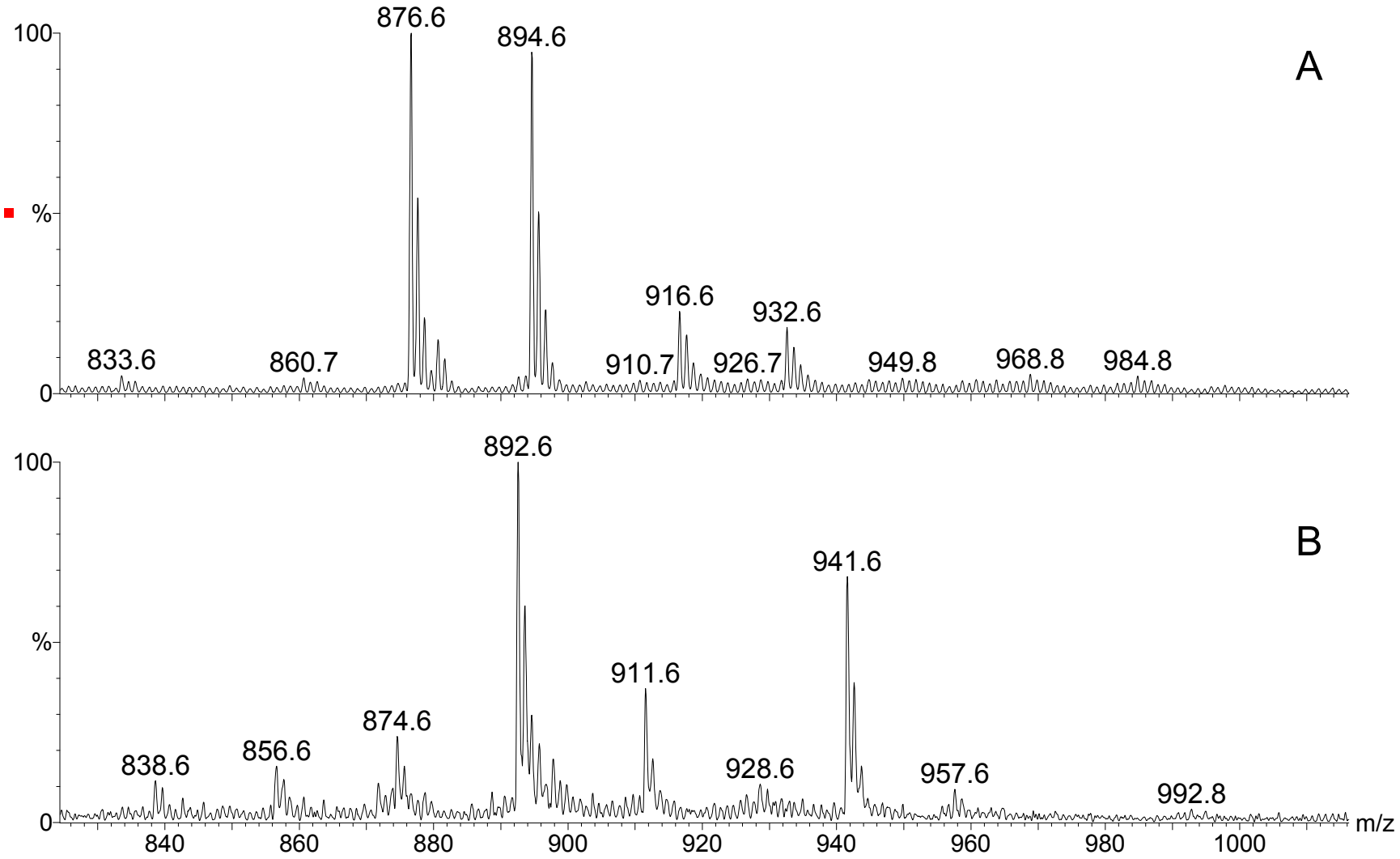
100
%
0
876.6
894.6
916.6
932.6
833.6
860.7
910.7
926.7
949.8
968.8
984.8
A
100
%
0
892.6
941.6
911.6
874.6
838.6
856.6
928.6
957.6
992.8
B
840
860
880
900
920
940
960
980
1000
m/z

Figure 7

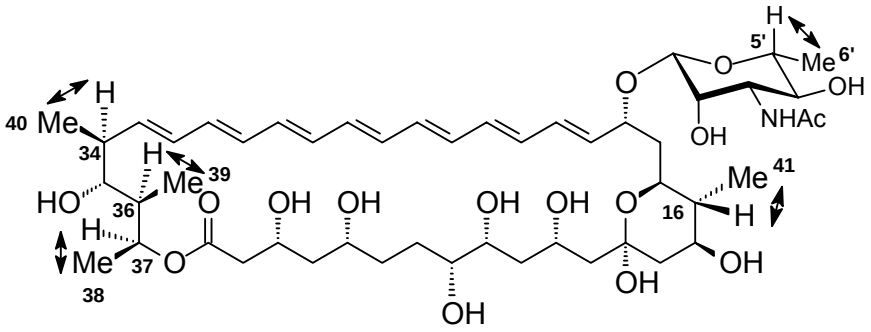
H
5'
Me
6'
O
O
OH
NHAc
OH
H
40
Me
34
H
Me
39
HO
36
O
OH
OH
OH
OH
O
16
Me
41
H
H
Me
37
O
38
OH
OH
OH

Figure 8A

S. nodosus

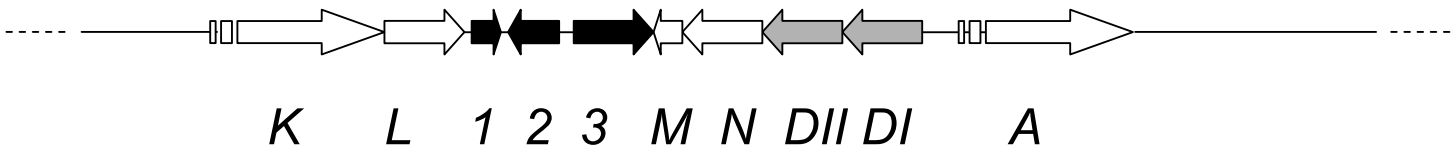

Lysogen

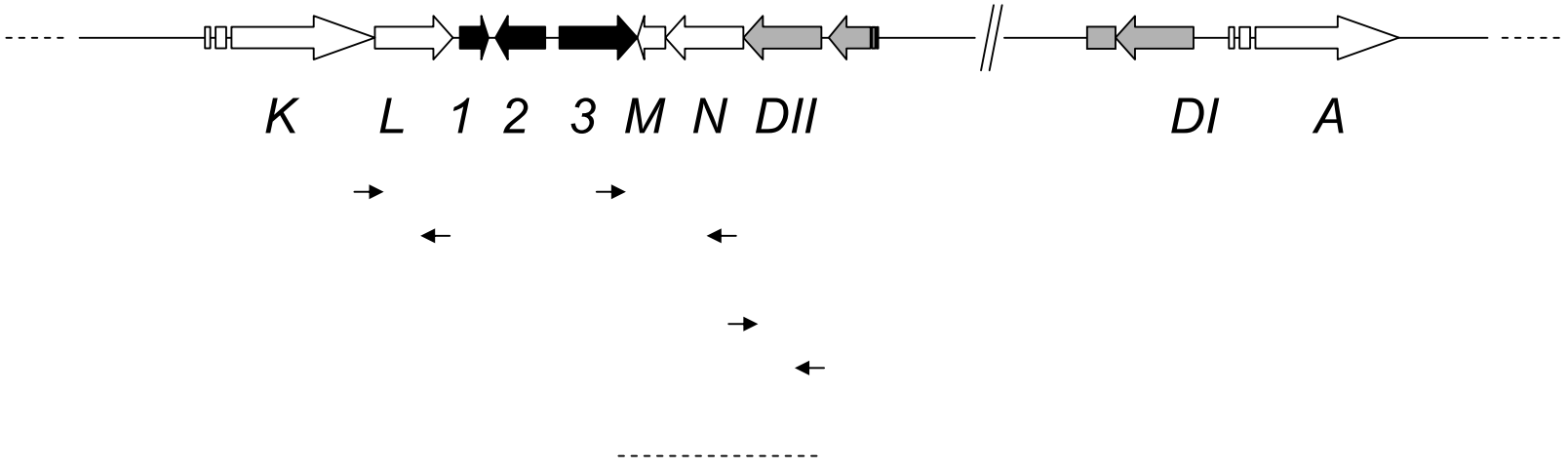

Region deleted in *S. nodosus DI-2*

Figure 8B

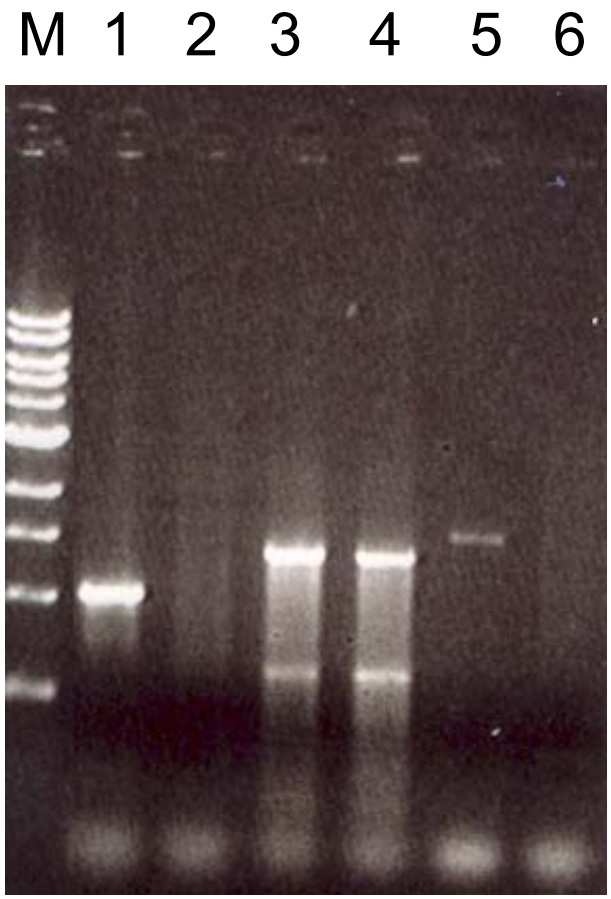

Figure 9

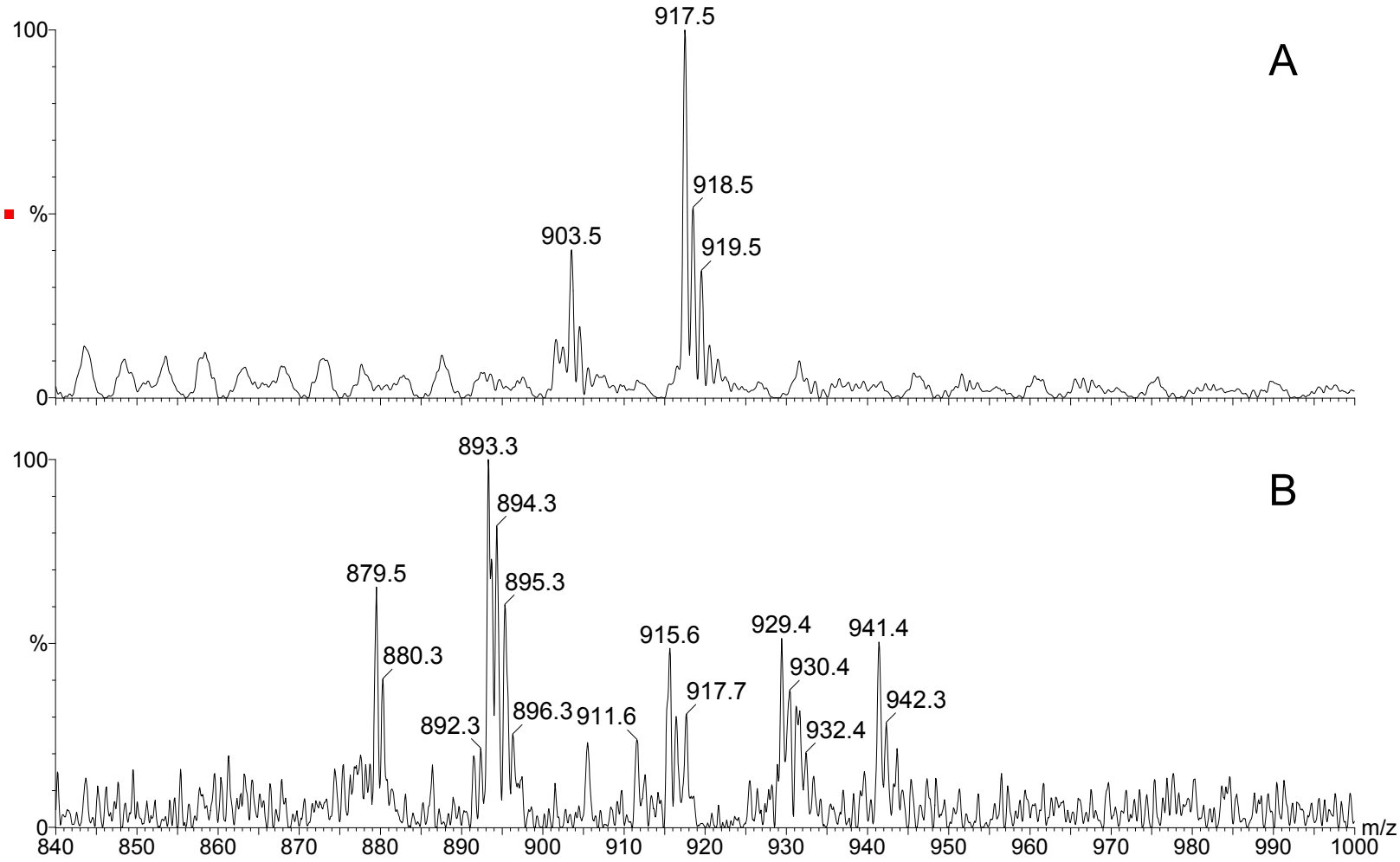
A
100
%
0
917.5
918.5
903.5
919.5
B
100
%
0
893.3
894.3
879.5
895.3
915.6
929.4
941.4
880.3
930.4
917.7
942.3
896.3
911.6
892.3
932.4
840
850
860
870
880
890
900
910
920
930
940
950
960
970
980
990
1000
m/z

Figure 10

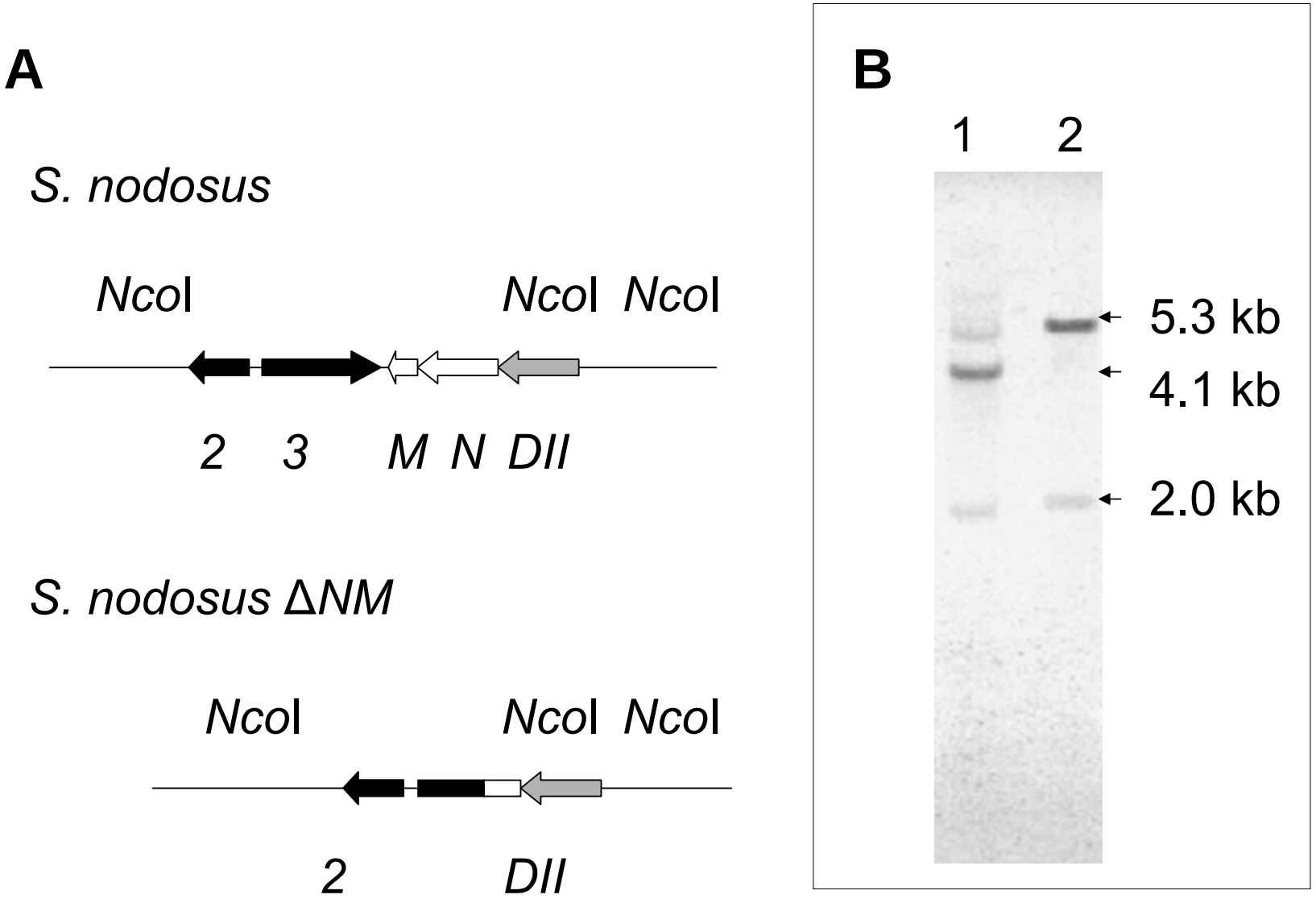
A
S. nodosus
NcoI
NcoI NcoI
2 3 M N DII
S. nodosus ΔNM
NcoI
NcoI NcoI
2 DII
B
1 2
5.3 kb
4.1 kb
2.0 kb

Figure 11

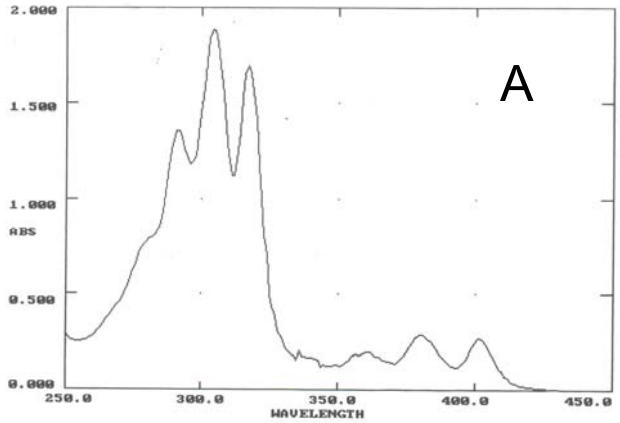
A
2.000
1.500
1.000
ABS
0.500
0.000
250.0
300.0
350.0
400.0
450.0
WAVELENGTH

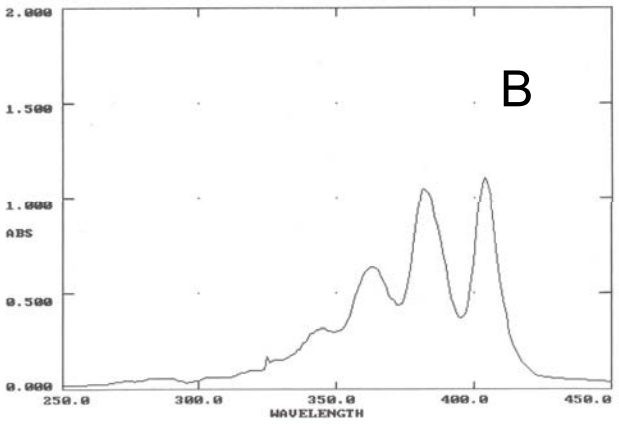
B
2.000
1.500
1.000
ABS
0.500
0.000
250.0
300.0
350.0
400.0
450.0
WAVELENGTH

Figure 12

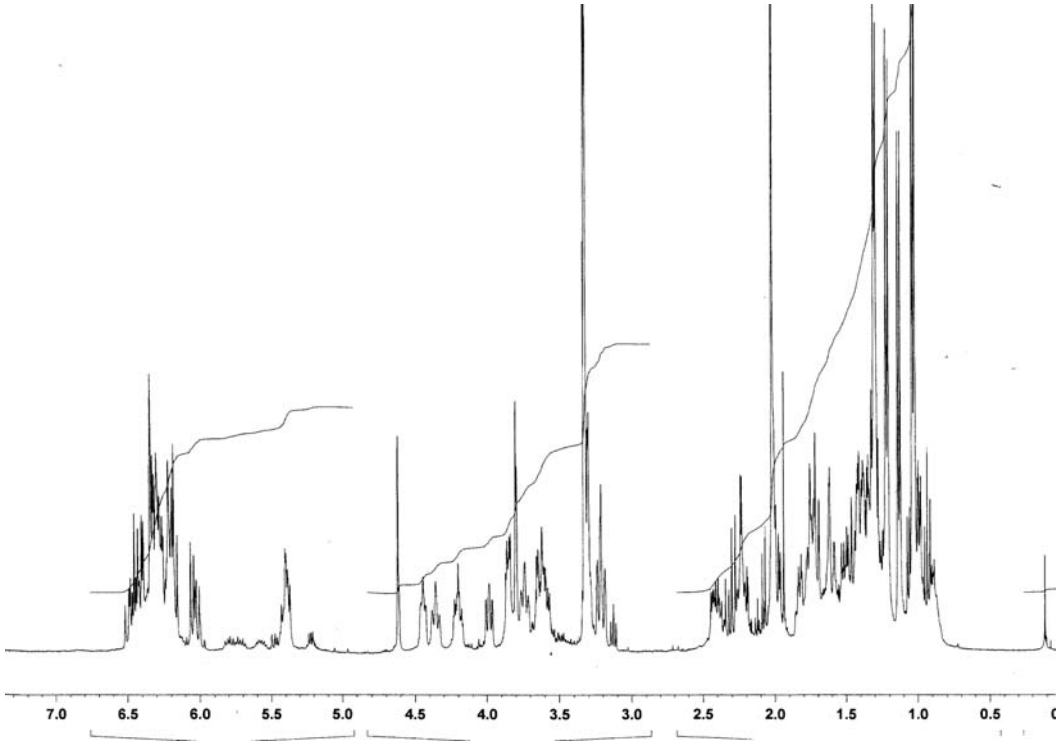

Figure 13

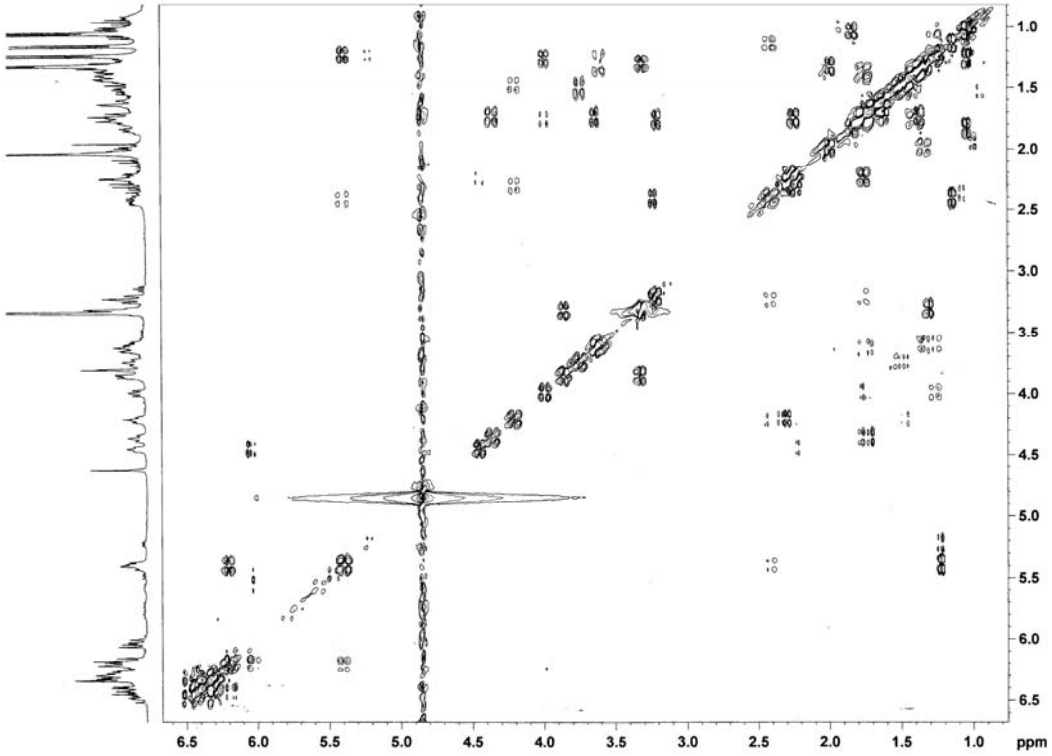
1.0
1.5
2.0
2.5
3.0
3.5
4.0
4.5
5.0
5.5
6.0
6.5
6.5
6.0
5.5
5.0
4.5
4.0
3.5
3.0
2.5
2.0
1.5
1.0
ppm